Dose-response Modeling of Nanomaterial Toxicity

Rahmasari Nur Azizah, Geert R. Verheyen, Sabine Van Miert and Ziv Shkedy

1. Introduction

2. Data

As an example of the application of the methodology, a dataset gathered in the NanoInformaTIX project (NanoInformaTIX, 2019) is used. The dataset is obtained from the NanoGenotox project on the eNanoMapper database (Jeliazkova, et al., 2015).

2.1 Data structure

The dataset used contains the result of the genetic in vitro studies of nanomaterial toxicity. It has a total number of observations equals to 30083. For the case study, the data obtained from NanoGenotox project is selected. The interest is in the measure of toxicity indicated by the DNA strand breaks, which is calculated by the percentage of the DNA in tail. Filtering the data according to the project source and the toxicity endpoint and after omitting the non-nanomaterials, the subset of the data from NanoGenotox project with endpoint DNA strand breaks is observed to have a total number of observations equals to 583 observations. It contains the data of Titanium Dioxide, Multi-walled carbon nanotubes, Synthetic Amorphous Silica, Zinc Oxide and control observations, as detailed in 1.

Table 1: Nanomaterials in the dataset

Nanomaterial	Number of observations
control	100
Control	32
medium	27
medium + BSA	33
NM-100 (Titanium Dioxide)	20
NM-102 (Titanium Dioxide, anatase)	58
NM-103 (Titanium Dioxide)	4
NM-104 (Titanium Dioxide)	5
NM-105 (Titanium Dioxide)	26
NM-110 (Zinc Oxide, uncoated)	158
NM-200 (Synthetic Amorphous Silica PR-A-02)	40
NM-203 (Synthetic Amorphous Silica PY-A-04)	40
NM-400 (Multi-walled carbon nanotubes)	40

2.2 Graphical display

In the dose-response relationship analysis, the response analyzed is the DNA strand breaks and the dose is the administered concentration of the nanomaterial. The DNA strand breaks is assumed to increase as the

concentration of the nanomaterial increases. An example of the plot of the dose and the response is in figure 1.

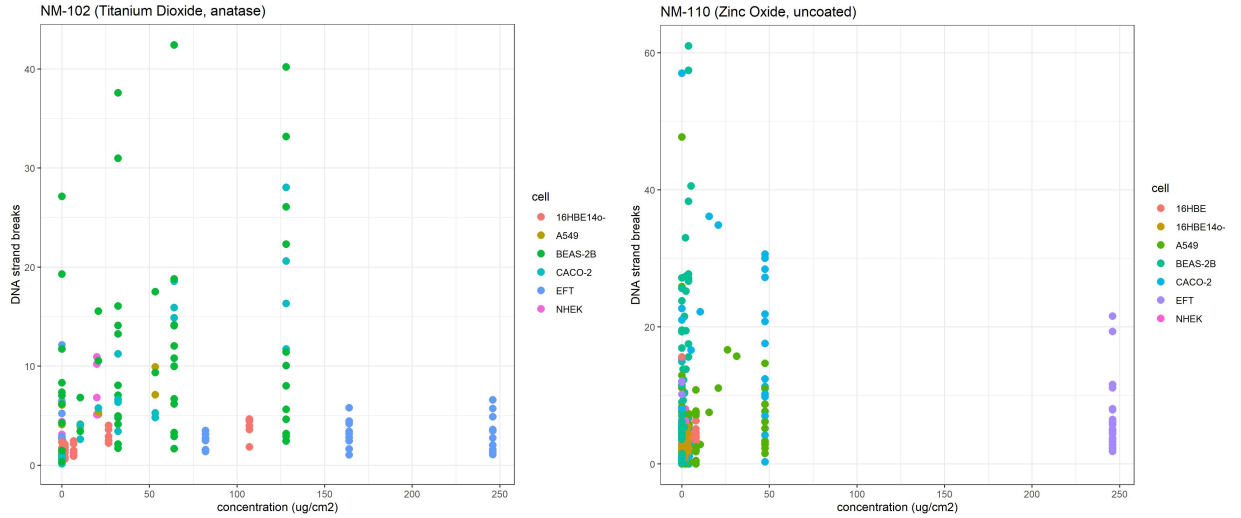

Figure 1: Plot of NM-102 and NM-110

Figure 1 shows the scatter plot of the DNA strand breaks and the concentration of the nanomaterial (in unit ug/cm2), differentiated by the cell types used in the experiment. As seen in the figure 1, for each nanomaterial, the experiments were performed on several different cell types.

3. Methodology

3.1 Inference for order restricted alternative

There are several methods that can be applied to test the monotonic trend of the means (Lin et al., 2012) such as the methods of Williams, and of Marcus which are t-tests for order restricted inference, and the likelihood ratio test which is discussed in Section 3.1.1.

3.1.1 Likelihood ratio test

One of the methods that can be used to test the equality of the mean response under order restriction is through a Likelihood ratio test. This test can be used to detect a monotone trend but cannot give an indication in which dose(s) there is a difference. The test statistics is given by:

$$\Lambda_{01}^{\frac{2}{N}} = \frac{\hat{\sigma}^2_{H_1}}{\hat{\sigma}^2_{H_0}} = \frac{\sum_{ij}(y_{ijm} - \hat{\mu}_i^\star)^2}{\sum_{ij}(y_{ijm} - \hat{\mu})^2}, \tag{1}$$

with $\hat{\mu} = \sum_{ij} y_{ij} / \sum_i n_i$. It is the ratio between error variance under H_0 and error variance under H_1. The test statistics can also be written in term of

$$\bar{E}^2_{01} = 1 - \Lambda_{01}^{\frac{2}{N}} \tag{2}$$

The null hypothesis is rejected for a large value of $\bar{E}^2_{01}$ or for a small value of $\Lambda_{01}^{\frac{2}{N}}$. When the direction of the trend is unknown, the more likely direction can be chosen by comparing likelihood of the increasing and decreasing trend, the direction with the higher likelihood is selected.

3.2 Non-linear Dose-response models

3.2.1 Model formulation

The log-logistic model

$$f(x) = c + \frac{d-c}{(1+exp(b(log(x)-log(e))))^f} \tag{3}$$

with
b: coefficient denoting the steepness of the dose-response curve
c: the lower asymptotes or limits of the response
d: the upper asymptotes or limits of the response
e: the effective dose ED50. f:
Fixing $f = 1$ results in 4 parameters log-logistic model, and fixing $f = 1$ and $c = 0$ results in 3 parameters log-logistic model.

Gompertz

$$f(x) = c + (d-c)(exp(-exp(b(x-e)))) \tag{4}$$

Weibull

$$f(x) = c + (d-c)exp(-exp(b(log(x)-log(e)))) \tag{5}$$

To estimate the parameters in the models, maximum likelihood estimation is used, which simplifies to nonlinear least squares under the assumption of normally distributed response. To obtain the nonlinear least squares estimates, the sum of squares in Eq ... needs to be minimized.

with w_i as the weight used to address the variance heterogeneity in the response. Eq ... is solved numerically in an iterative manner, using a general-purpose minimizer. The scaled inverse of the observed information matrix is used to estimate the variance-covariance of the parameter estimates (cov()), as follows:

3.2.2 Estimation of effective dose

The effective doses can be estimated using inverse regression. An example of the effective doses that can be derived is ED50, which is the dose that is associated with a halfway reduction between the lower and the upper limits of the dose-response curve f as doses approach infinity and 0, respectively. The effective dose for $0 < \alpha < 1(ED100\alpha)$ for a decreasing mean function f is the solution of

$$f(ED100\alpha, \beta) = (1-\alpha)\lim_{x\to 0} f(x,\beta) + \alpha \lim_{x\to\infty} f(x,\beta) = (1-\alpha)c + \alpha d \tag{6}$$

3.3 Model Averaging

To incorporate the model selection uncertainty into the inference, a model-averaged effective dose can be estimated. Suppose that there are K models, M_i, $i = 1, \ldots, K$, and θ is the parameter of the effective dose. Let $\hat{\theta}_i$ be the estimate of the effective dose for model M_i. The estimated model-averaged effective dose can be calculated as

$$\hat{\theta} = \sum_{i=1}^{K} w_i \hat{\theta}_i \tag{7}$$

which is the weighted average of $\hat{\theta}_i$. The weight for model M_i is denoted by w_i which equals to

$$w_i = \frac{exp(-I_i/2)}{\sum_{j=1}^{K} exp(-I_j/2)} \tag{8}$$

with $i = 1, \ldots, K$ and $\sum_{i=1}^{K} w_i = 1$. I is the Akaike's Information Criterion (AIC) that can be calculated by $I = -2L + 2h$, with L the log-likelihood function and h the number of parameters.

4. Application to the Data

Following the data exploration, inference for order restricted alternative was performed to investigate significant monotonic trend on the dose-response relationship of nanomaterial toxicity.

4.1 Trend

Figure 2 shows the plot of the DNA strand breaks and the concentration of the nanomaterial with isotonic means, for NM-102 (Titanium Dioxide, anatase) and NM-110 (Zinc Oxide, uncoated), for 16HBE14o- and CACO-2 cell type respectively.

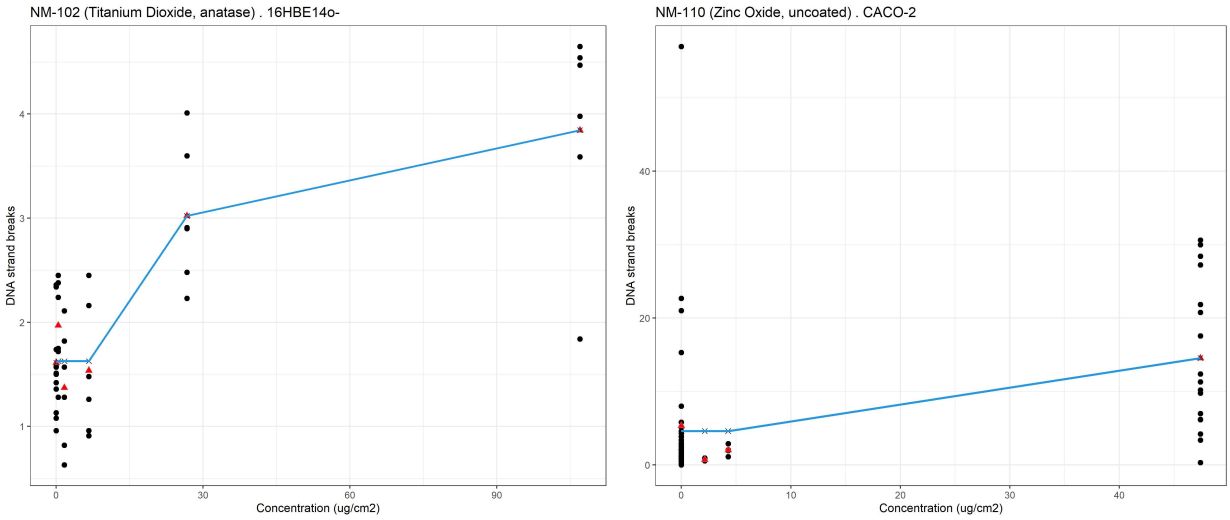

Figure 2: Isotonic means plot of NM-102 and NM-110

Differentiating the data for each nanomaterial according to the cell types resulted in 65 subsets of data. Among these 65 subsets of data, using Likelihood ratio test, significant trend was found on 16 data subsets as seen in table 2.

Table 2: Nanomaterials with significant trend

Nanomaterial	Cell type	E2	p-value	adjusted p-value
NM-103 (Titanium Dioxide)	NHEK	0.584	0.000	0.000
NM-400 (Multi-walled carbon nanotubes)	CACO-2	0.205	0.002	0.009
NM-105 (Titanium Dioxide)	16HBE14o-	0.715	0.000	0.000
NM-105 (Titanium Dioxide)	NHEK	0.622	0.011	0.045
NM-200 (Synthetic Amorphous Silica PR-A-02)	16HBE	0.200	0.001	0.005
NM-203 (Synthetic Amorphous Silica PY-A-04)	BEAS-2B	0.322	0.001	0.005
NM-100 (Titanium Dioxide)	16HBE14o-	0.670	0.000	0.000
NM-102 (Titanium Dioxide, anatase)	16HBE14o-	0.647	0.000	0.000
NM-102 (Titanium Dioxide, anatase)	A549	0.751	0.011	0.045
NM-102 (Titanium Dioxide, anatase)	CACO-2	0.812	0.000	0.000
NM-102 (Titanium Dioxide, anatase)	NHEK	0.633	0.000	0.000
NM-104 (Titanium Dioxide)	NHEK	0.626	0.000	0.000
NM-110 (Zinc Oxide, uncoated)	16HBE14o-	0.160	0.001	0.005
NM-110 (Zinc Oxide, uncoated)	BEAS-2B	0.297	0.000	0.000
NM-110 (Zinc Oxide, uncoated)	CACO-2	0.182	0.000	0.000

NM-110 (Zinc Oxide, uncoated)	NHEK	0.631	0.000		0.000

Further analysis on the dose-response relationship, which is fitting the non-linear models can be performed on these subsets of data in which significant monotonic trend was found.

4.2 Dose-response model fitting

As an illustration for the dose-response analysis, data subsets of Nanomaterial NM-102 (Titanium Dioxide, anatase) and NM-110 (Zinc Oxide, uncoated) are selected. The data subset of NM-102 (Titanium Dioxide, anatase) contains the result of experiment performed on 16HBE14o- cell type with a total number of observations 42 observations, while the data subset of NM-110 (Zinc Oxide, uncoated) consists of 67 observations on the CACO-2 cell type.

Table 3: Estimate of ED50 of NM-102 (Titanium Dioxide, anatase) with cell type 16HBE14o-

	Estimate	Standard error	Lower	Upper	AIC	Weight
4PL	24.353	7.651	8.864	39.842	89.944	0.348
5PL	23.735	27.137	0.000	78.721	91.942	0.128
Weibull	22.710	9.448	3.584	41.836	89.941	0.348
Gompertz	7.403	30.062	0.000	68.210	91.312	0.176

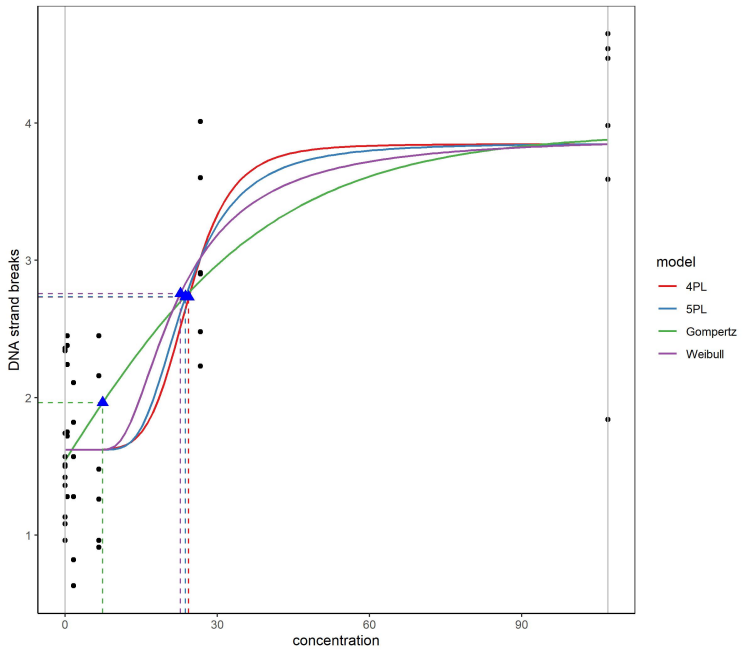

Figure 3: Dose-response plot of NM-102

Table 4: Estimate of ED50 of NM-110 (Zinc Oxide, uncoated) with cell type CACO-2.ug/cm2

	Estimate	Standard error	Lower	Upper	AIC	Weight

3PL	4.730	0.515	3.702	5.758	511.740	0.009
4PL	4.888	0.586	3.717	6.060	504.274	0.369
5PL	4.851	0.822	3.208	6.494	506.243	0.138
Weibull	4.764	0.774	3.218	6.311	504.250	0.373
Gompertz	3.647	7.495	0.000	18.619	506.660	0.112

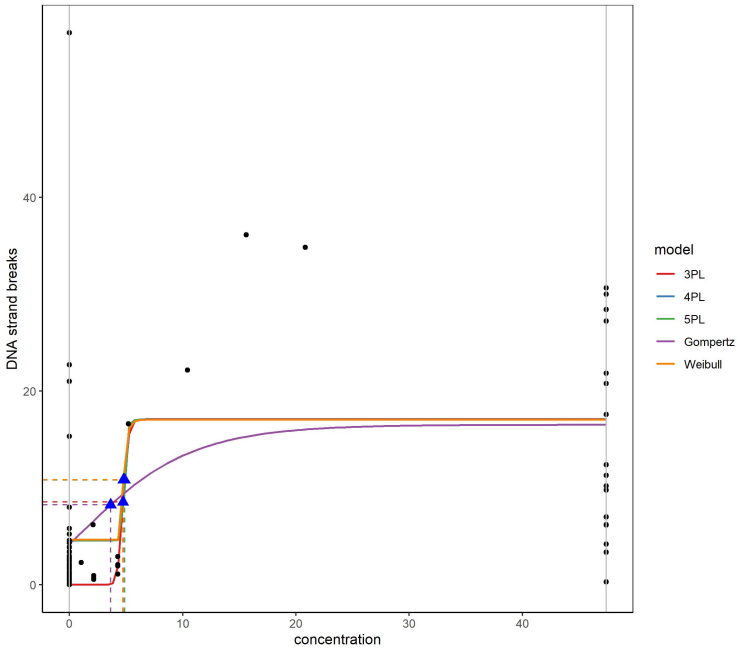

Figure 4: Dose-response plot of NM-110

5. Discussion

References

Appendix

Table 5: Test statistics and p-values for all data subsets

name	Cell type	E2	p-value	adjusted p-value
NM-103 (Titanium Dioxide)	16HBE14o-	0.144	0.109	0.291
NM-103 (Titanium Dioxide)	A549	0.173	0.277	0.462
NM-103 (Titanium Dioxide)	BEAS-2B	0.578	0.066	0.215
NM-103 (Titanium Dioxide)	CACO-2	0.769	0.014	0.054
NM-103 (Titanium Dioxide)	EFT	0.000	0.752	0.786
NM-103 (Titanium Dioxide)	NHEK	0.584	0.000	0.000
NM-400 (Multi-walled carbon nanotubes)	16HBE	0.004	0.481	0.665
NM-400 (Multi-walled carbon nanotubes)	A549	0.000	0.649	0.725
NM-400 (Multi-walled carbon nanotubes)	BEAS-2B	0.047	0.257	0.462
NM-400 (Multi-walled carbon nanotubes)	CACO-2	0.205	0.002	0.009
NM-401 (Multi-walled carbon nanotubes)	16HBE	0.010	0.360	0.571
NM-401 (Multi-walled carbon nanotubes)	A549	0.000	0.653	0.725
NM-401 (Multi-walled carbon nanotubes)	BEAS-2B	0.024	0.523	0.705
NM-401 (Multi-walled carbon nanotubes)	CACO-2	0.011	0.577	0.705
NM-402 (Multi-walled carbon nanotubes)	16HBE	0.001	0.581	0.705
NM-402 (Multi-walled carbon nanotubes)	A549	0.001	0.605	0.705
NM-402 (Multi-walled carbon nanotubes)	BEAS-2B	0.144	0.146	0.351
NM-402 (Multi-walled carbon nanotubes)	CACO-2	0.025	0.448	0.657
NM-105 (Titanium Dioxide)	16HBE14o-	0.715	0.000	0.000
NM-105 (Titanium Dioxide)	A549	0.433	0.105	0.291
NM-105 (Titanium Dioxide)	BEAS-2B	0.271	0.237	0.440
NM-105 (Titanium Dioxide)	CACO-2	0.276	0.201	0.408
NM-105 (Titanium Dioxide)	EFT	0.000	0.765	0.786
NM-105 (Titanium Dioxide)	NHEK	0.622	0.011	0.045
NM-200 (Synthetic Amorphous Silica PR-A-02)	16HBE	0.200	0.001	0.005
NM-200 (Synthetic Amorphous Silica PR-A-02)	A549	0.143	0.034	0.123
NM-200 (Synthetic Amorphous Silica PR-A-02)	BEAS-2B	0.149	0.137	0.342
NM-200 (Synthetic Amorphous Silica PR-A-02)	CACO-2	0.016	0.433	0.655
NM-203 (Synthetic Amorphous Silica PY-A-04)	16HBE	0.019	0.465	0.657
NM-203 (Synthetic Amorphous Silica PY-A-04)	A549	0.022	0.459	0.657
NM-203 (Synthetic Amorphous Silica PY-A-04)	BEAS-2B	0.322	0.001	0.005
NM-203 (Synthetic Amorphous Silica PY-A-04)	CACO-2	0.055	0.192	0.403
NM-100 (Titanium Dioxide)	16HBE14o-	0.670	0.000	0.000
NM-102 (Titanium Dioxide, anatase)	16HBE14o-	0.647	0.000	0.000
NM-102 (Titanium Dioxide, anatase)	A549	0.751	0.011	0.045
NM-102 (Titanium Dioxide, anatase)	BEAS-2B	0.066	0.112	0.291
NM-102 (Titanium Dioxide, anatase)	CACO-2	0.812	0.000	0.000
NM-102 (Titanium Dioxide, anatase)	EFT	0.000	0.774	0.786
NM-102 (Titanium Dioxide, anatase)	NHEK	0.633	0.000	0.000
NM-104 (Titanium Dioxide)	16HBE14o-	0.000	0.808	0.808
NM-104 (Titanium Dioxide)	A549	0.095	0.389	0.602
NM-104 (Titanium Dioxide)	BEAS-2B	0.208	0.277	0.462
NM-104 (Titanium Dioxide)	CACO-2	0.214	0.277	0.462
NM-104 (Titanium Dioxide)	EFT	0.090	0.188	0.403
NM-104 (Titanium Dioxide)	NHEK	0.626	0.000	0.000

NM-101 (Titanium Dioxide)	16HBE14o-	0.166	0.084	0.260
NM-201 (Synthetic Amorphous Silica PR-B-01)	16HBE	0.011	0.538	0.705
NM-201 (Synthetic Amorphous Silica PR-B-01)	A549	0.007	0.607	0.705
NM-201 (Synthetic Amorphous Silica PR-B-01)	BEAS-2B	0.005	0.741	0.786
NM-201 (Synthetic Amorphous Silica PR-B-01)	CACO-2	0.126	0.055	0.188
NM-202 (Synthetic Amorphous Silica PY-AB-03)	16HBE	0.031	0.346	0.562
NM-202 (Synthetic Amorphous Silica PY-AB-03)	A549	0.095	0.107	0.291
NM-202 (Synthetic Amorphous Silica PY-AB-03)	BEAS-2B	0.111	0.218	0.417
NM-202 (Synthetic Amorphous Silica PY-AB-03)	CACO-2	0.066	0.164	0.368
NM-403 (Multi-walled carbon nanotubes)	16HBE	0.000	0.597	0.705
NM-403 (Multi-walled carbon nanotubes)	A549	0.000	0.658	0.725
NM-403 (Multi-walled carbon nanotubes)	BEAS-2B	0.008	0.564	0.705
NM-403 (Multi-walled carbon nanotubes)	CACO-2	0.004	0.753	0.786
NM-110 (Zinc Oxide, uncoated)	16HBE	0.022	0.218	0.417
NM-110 (Zinc Oxide, uncoated)	16HBE14o-	0.160	0.001	0.005
NM-110 (Zinc Oxide, uncoated)	A549	0.030	0.158	0.367
NM-110 (Zinc Oxide, uncoated)	BEAS-2B	0.297	0.000	0.000
NM-110 (Zinc Oxide, uncoated)	CACO-2	0.182	0.000	0.000
NM-110 (Zinc Oxide, uncoated)	EFT	0.000	0.554	0.705
NM-110 (Zinc Oxide, uncoated)	NHEK	0.631	0.000	0.000